ACS POLYMERS Au
AN OPEN ACCESS JOURNAL OF THE AMERICAN CHEMICAL SOCIETY

pubs.acs.org/polymerau
Article

Ampholytic Peptides Consisting of an Alternating Lysine/Glutamic Acid Sequence for the Simultaneous Formation of Polyion Complex Vesicles

Kousuke Tsuchiya,* Seiya Fujita, and Keiji Numata*

Cite This: ACS Polym. Au 2024, 4, 320−330
Read Online

ACCESS | Metrics & More | Article Recommendations | Supporting Information

ABSTRACT: Nanoarchitectures such as micelles and vesicles that self-assemble via electrostatic interactions between their charged polymeric components have been widely used as material delivery platforms. In this work, ampholytic peptides with a sequence of alternating lysine and glutamic acid residues were designed and synthesized via chemoenzymatic polymerization. This alternating sequence was achieved by trypsin-catalyzed polymerization of a dipeptide monomer. Due to the electrostatic interaction between the anionic and cationic residues, the prepared ampholytic peptides spontaneously formed nanosized assemblies with a size of 100−200 nm in water. Modification with tetra(ethylene glycol) (TEG) at the *N*-terminus of these ampholytic alternating peptides resulted in the formation of stable nanosized assemblies, while peptides consisting of random sequences of lysine and glutamic acid formed large aggregates with deteriorated stability even with TEG modification. Morphological observations using a field-emission scanning electron microscope and an atomic force microscope revealed that the obtained assemblies were spherical and hollow, indicating the spontaneous formation of vesicles from the TEG-modified ampholytic alternating peptides. These vesicles were able to encapsulate a model fluorescent protein within their hollow structures without structural collapse causing loss of fluorescence, demonstrating the potential of these nanocarriers for use in material delivery systems.

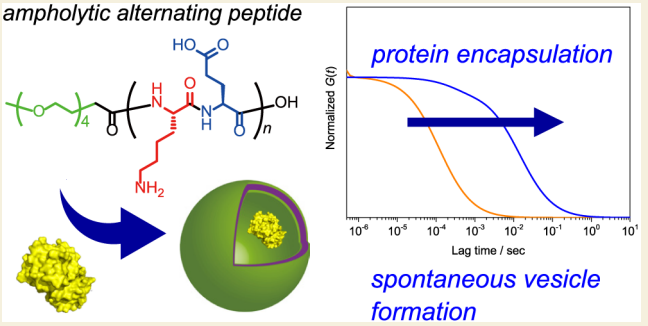

KEYWORDS: *ampholyte, peptide, self-assembly, vesicle, protein encapsulation*

With a combination of opposite charges, both biomolecules and synthetic molecules exploit electrostatic interactions to undergo self-assembly to construct myriad complexes with unique sizes and morphologies that result in specific functions. In living systems, charged amino acids in proteins/peptides play critical roles, such as providing scaffolds for proton transfer in response to pH changes, serving as reaction centers in enzymes, and functionalizing and stabilizing higher-order structures. A reversible ionic bond can form between anionic and cationic amino acids, such as lysine (Lys) and glutamic acid (Glu)/aspartic acid (Asp), that contributes to the formation of various protein structures/assemblies.[1−3] The electrostatic interactions between charged amino acid residues have been exploited for the production of various artificial assemblies with specific properties. Polypeptides containing lysine and glutamic acid residues have been utilized to assemble fibers, lamellar nanosheets, and micellar particles for applications in various fields.[4−8] For example, de novo-designed self-assembling peptides containing Lys and Glu residues were assembled into β-sheet nanofibers, which then formed protein-fused supramolecular architectures with biological functions in living cells.[4]

The coexistence of Lys and Glu residues imparts ampholytic properties to proteins/polypeptides. The most important feature of ampholytic polymeric materials is their resistance to nonspecific interactions with biomolecules.[9−11] Recent research has revealed that chaperone proteins, whose interior can resist nonspecific interactions with target proteins, have abundant ampholytic combinations of Lys and Glu residues on their inner surface.[12] Inspired by this finding, researchers have developed artificial polypeptides containing an alternating sequence of Lys and Glu for use as antifouling coating materials.[13−18]

Polyion complexes composed of polyanions and polycations have been widely utilized for the assembly of various architectures. Nanoassemblies with a micellar or vesicular morphology have been prepared by mixing polymeric

Received: March 26, 2024
Revised: May 8, 2024
Accepted: May 9, 2024
Published: May 29, 2024

https://doi.org/10.1021/acspolymersau.4c00029
ACS Polym. Au 2024, 4, 320−330

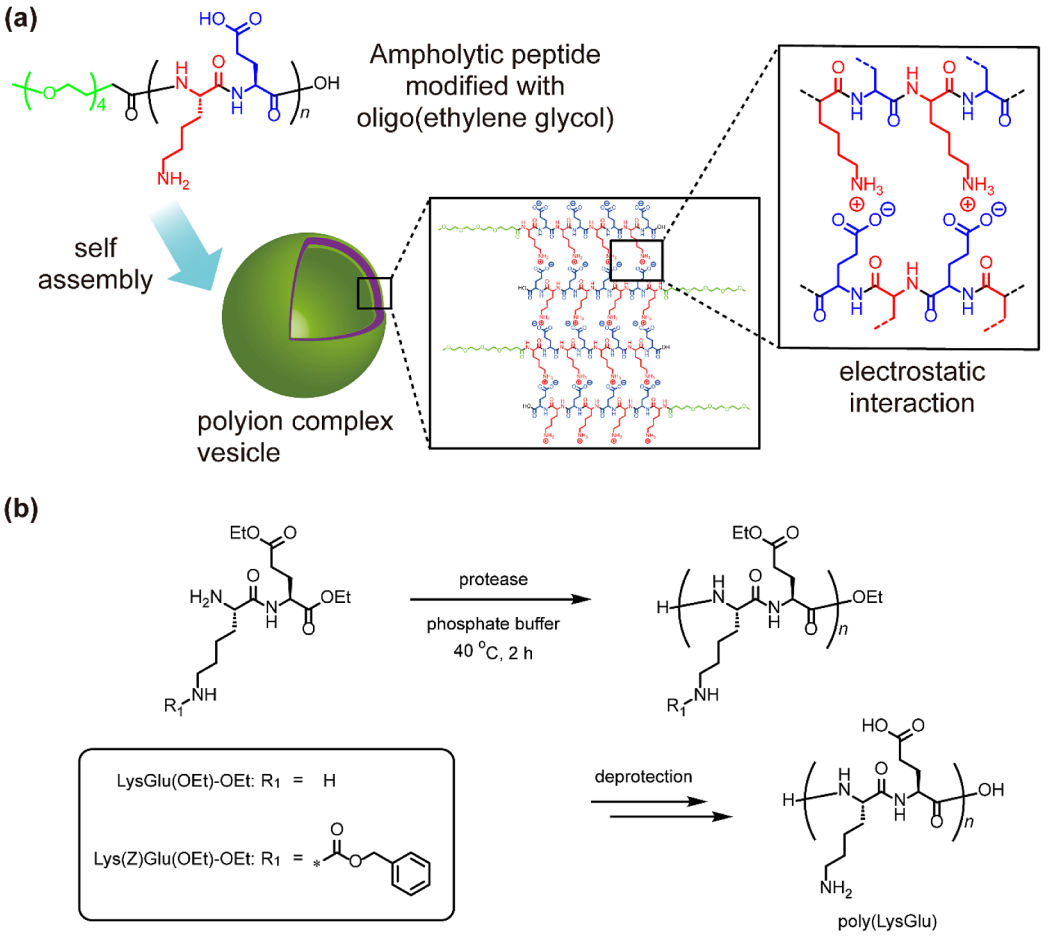

Figure 1. Synthesis and self-assembly of a peptide with a LysGlu alternating sequence. (a) Schematic illustration of vesicle formation through the self-assembly of an oligo(ethylene glycol)-modified ampholytic peptide with a LysGlu alternating sequence. (b) Scheme of the synthesis of poly(LysGlu) by protease-catalyzed polymerization followed by deprotection of the side groups.

components with equimolar anionic and cationic charges and have been applied as nanocarriers for material delivery in living systems.[19] In particular, polyion complex vesicles, termed polyion complexsomes (PICsomes), have been developed as polymeric carriers, and various biomolecules, such as proteins, have been incorporated into their internal cavities.[20−23] Cargo materials can retain their functional structures and physiological functions within the cavity of PICsomes. Therefore, these cargos can exert their intended functions at the specific sites where they are delivered by the PICsome carriers. Previously, we reported that a combination of short oligopeptides with anionic and cationic residues was applied to form vesicular assemblies.[24−26] This peptide-based PICsome encapsulating a protein/DNA was successfully used to deliver cargo protein into plant cells.

The synthesis of peptides with functional sequences via solid-phase peptide synthesis (SPPS), where peptide elongation occurs via stepwise condensation on solid supports, has been well established. SPPS allows precise control of complex peptide sequences, although limitations in terms of peptide length and large-scale production exist. On the other hand, peptides with periodic sequences, including alternating peptides, are more accessible than peptides with complex sequences via solution-phase peptide synthesis. We and other groups have developed a chemoenzymatic peptide synthesis method using repeated aminolysis reactions of amino acid ester monomers mediated by proteases.[27−31] This enzymatic synthesis of peptides is an environmentally benign process and offers synthetic benefits in terms of stereo- and regioselectivity.[32] This method is applicable to the polymerization of oligopeptide ester monomers, resulting in the formation of peptides with various periodic sequences. In this study, we employed this chemoenzymatic approach to construct alternating peptides consisting of Lys and Glu residues. The alternating sequence, which was achieved by utilizing the corresponding dipeptide monomer, enabled the equimolar incorporation of anionic and cationic residues within peptide sequences. We successfully synthesized LysGlu alternating peptides via chemoenzymatic polymerization, followed by subsequent postmodification with an oligo(ethylene glycol) moiety. The resulting oligo(ethylene glycol)-modified alternating peptide was found to spontaneously assemble into vesicular particles via electrostatic interactions (Figure 1a).

RESULTS AND DISCUSSION

Chemoenzymatic Synthesis of LysGlu Alternating Polypeptides and Their Characterization

Chemoenzymatic polymerization of LysGlu dipeptide monomers using proteases was performed to synthesize ampholytic oligopeptides with a specific alternating sequence. During chemoenzymatic polymerization, ester derivatives of amino

https://doi.org/10.1021/acspolymersau.4c00029
ACS Polym. Au 2024, 4, 320−330

acids as monomers undergo continuous protease-catalyzed aminolysis reactions to afford the corresponding polypeptides. Oligopeptide esters consisting of two or more amino acids also polymerize in the presence of proteases, resulting in the formation of polypeptides with periodic amino acid sequences.[28−31] The selection of an appropriate protease is a key factor for controlling the polymerization because the substrate specificity of the proteases limits the range of valid reactants as acyl donors and nucleophiles. We selected papain and trypsin, which are categorized as cysteine proteases and serine proteases, respectively, as representative enzymes for the chemoenzymatic polymerization of LysGlu monomers. Papain exhibits relatively broad substrate specificity, favoring aromatic amino acid residues. Previously, papain-catalyzed polymerization was conducted for both Lys and Glu ester monomers, demonstrating the good affinity of papain for these amino acids.[33−35] On the other hand, trypsin has a high affinity for basic amino acid residues such as lysine and arginine.

Two types of LysGlu monomers were synthesized by conventional solution-phase synthesis: LysGlu(OEt)-OEt and Lys(Z)Glu(OEt)-OEt (Scheme S1, Figures S1−4). These dipeptide esters were applied to papain- or trypsin-catalyzed polymerization in aqueous buffers at a moderate temperature (Figure 1b). The results are summarized in Table 1. When the

Table 1. Chemoenzymatic Polymerization of LysGlu Dipeptide Ester Monomers.[a]

run	monomer	enzyme	yield[b]	sequence[c]
1	LysGlu(OEt)-OEt	papain	8.2	random
2	LysGlu(OEt)-OEt	trypsin	3.8	random
3	Lys(Z)Glu(OEt)-OEt	papain	48.6	random
4	Lys(Z)Glu(OEt)-OEt	trypsin	91.3	alternating
5	Lys(Z)Glu(OEt)-OEt	bromelain	57.2	random

[a]Polymerization was carried out using LysGlu(OEt)-OEt or Lys(Z)-Glu(OEt)-OEt HCl salt (0.1 M) and enzyme (50 mg/mL) in phosphate buffer (1 M, pH 8.0) at 40 °C for 2 h. [b]The insoluble part was collected by centrifugation. [c]Estimated from the ^{1}H NMR and MALDI-TOF MS spectra.

polymerization of LysGlu(OEt)-OEt was carried out in the presence of papain or trypsin, a white precipitate gradually formed after 2 h (Runs 1 and 2). However, the yields of the precipitates were very low, at 8.2% and 3.8%, respectively. The obtained polypeptides were characterized by ^{1}H NMR spectroscopy and MALDI-TOF MS spectrometry. The MALDI-TOF MS spectra of poly[LysGlu(OEt)] showed multiple series of peaks that were attributed to polypeptides with various Lys/Glu compositions (Figure S5). In addition to the series of polypeptides with an equimolar Lys/Glu composition, polypeptides with sequences rich in Glu residues were observed by MALDI-TOF MS analysis (there were up to 4 Lys residues less in this sequence than in the completely alternating sequence). This result was probably due to the transamidation[27,29] or hydrolysis of the Lys-Glu peptide bond in both the LysGlu(OEt)-OEt monomer and the generated poly[LysGlu(OEt)]. The Lys-rich peptides were more water soluble, resulting in an enrichment of Glu-rich sequences in the low-yield precipitate. The ^{1}H NMR spectrum of poly[LysGlu-(OEt)] also provided evidence for the formation of Glu-rich randomized sequences (Figure S6). The signal attributed to the methylene protons of the Glu unit at 2.3 ppm was 1.3 times more intense than that attributed to the methylene protons of the Lys unit at 2.9 ppm. Therefore, a highly randomized sequence structure was obtained via the chemoenzymatic polymerization of LysGlu(OEt)-OEt.

Chemoenzymatic polymerization of the Lys(Z)Glu(OEt)-OEt monomer was also performed using different proteases (Runs 3−5). A benzyloxycarbonyl (Z) substituent on the side chain of the Lys residue increased the hydrophobicity of the polypeptide. For the protease-catalyzed polymerization of Lys(Z)Glu(OEt)-OEt, the yield of the precipitate was drastically increased, especially for the trypsin-catalyzed polymerization. The papain-catalyzed polymerization afforded the precipitate in 48.6% yield, whereas the yield of the precipitate reached 91.3% for trypsin-catalyzed polymerization.

The MALDI-TOF MS spectra of the polypeptides differed depending on the protease used. The spectrum of the polypeptide synthesized using papain showed a major series of peaks attributed to poly[Lys(Z)Glu(OEt)] with an equimolar Lys/Glu composition, accompanied by the peaks attributed to poly[Lys(Z)Glu(OEt)] with extra Glu addition or deletion (Figure 2a). The insertion or deletion of Glu residues was attributed to the scrambling of the sequence during papain-catalyzed polymerization via transamidation. In contrast, the spectrum of the polypeptide synthesized via trypsin-catalyzed polymerization showed only a series of peaks attributed to poly[Lys(Z)Glu(OEt)] with an equimolar Lys/Glu composition (Figure 2b). These results indicated that trypsin can appropriately recognize the LysGlu monomer sequence in its catalytic pocket. We also attempted to use bromelain, a cysteine protease in the same enzymatic category as papain, for the polymerization of Lys(Z)Glu(OEt)-OEt (Run 5 in Table 1). The polypeptide was obtained as a precipitate in good yield (57.2%), but the MALDI-TOF MS spectrum of the polypeptide also showed a series of peaks attributed to the scrambled sequences. In the substrate pocket of papain and bromelain, the amide bonds of the LysGlu monomers/units tended to react with the catalytic center, competing with the activation of the terminal ester group and thus resulting in sequence scrambling by transamidation.

The ^{1}H NMR spectra of the polypeptides obtained via papain- and trypsin-catalyzed polymerizations showed similar signals (Figure 2c,d). Slight differences in the spectra were observed, such as broadening of the methylene peak of the Glu unit at 2.3 ppm in the spectrum of the polypeptide obtained by papain-catalyzed polymerization, highlighting the difference in the randomness of the sequence. By comparing the signals at 2.3 and 2.9 ppm, the Lys/Glu compositions of the polypeptides were estimated to be 0.99 and 0.97 for papain- and trypsin-catalyzed polymerizations, respectively. Both polypeptides had equimolar Lys/Glu compositions even though the sequence was randomized after papain-catalyzed polymerization.

The two types of poly[Lys(Z)Glu(OEt)] with alternating or randomized sequences were deprotected by treatment with hydrobromic acid followed by hydrolysis with sodium hydroxide, affording polyLysGlu with unprotected side groups (Scheme S2). The chemical structure was confirmed by ^{1}H NMR spectroscopy, where the signals of the ethyl ester and Z groups completely disappeared (Figure 2e). Hereafter, the polypeptides with alternating and randomized LysGlu sequences are denoted as polyKE^{alt} and polyKE^{ran}, respectively.

The secondary structures of polyKE^{alt} and polyKE^{ran} were investigated by circular dichroism (CD) spectroscopy (Figure 3). The CD spectrum of polyKE^{alt} polymerized using trypsin

https://doi.org/10.1021/acspolymersau.4c00029
ACS Polym. Au 2024, 4, 320−330

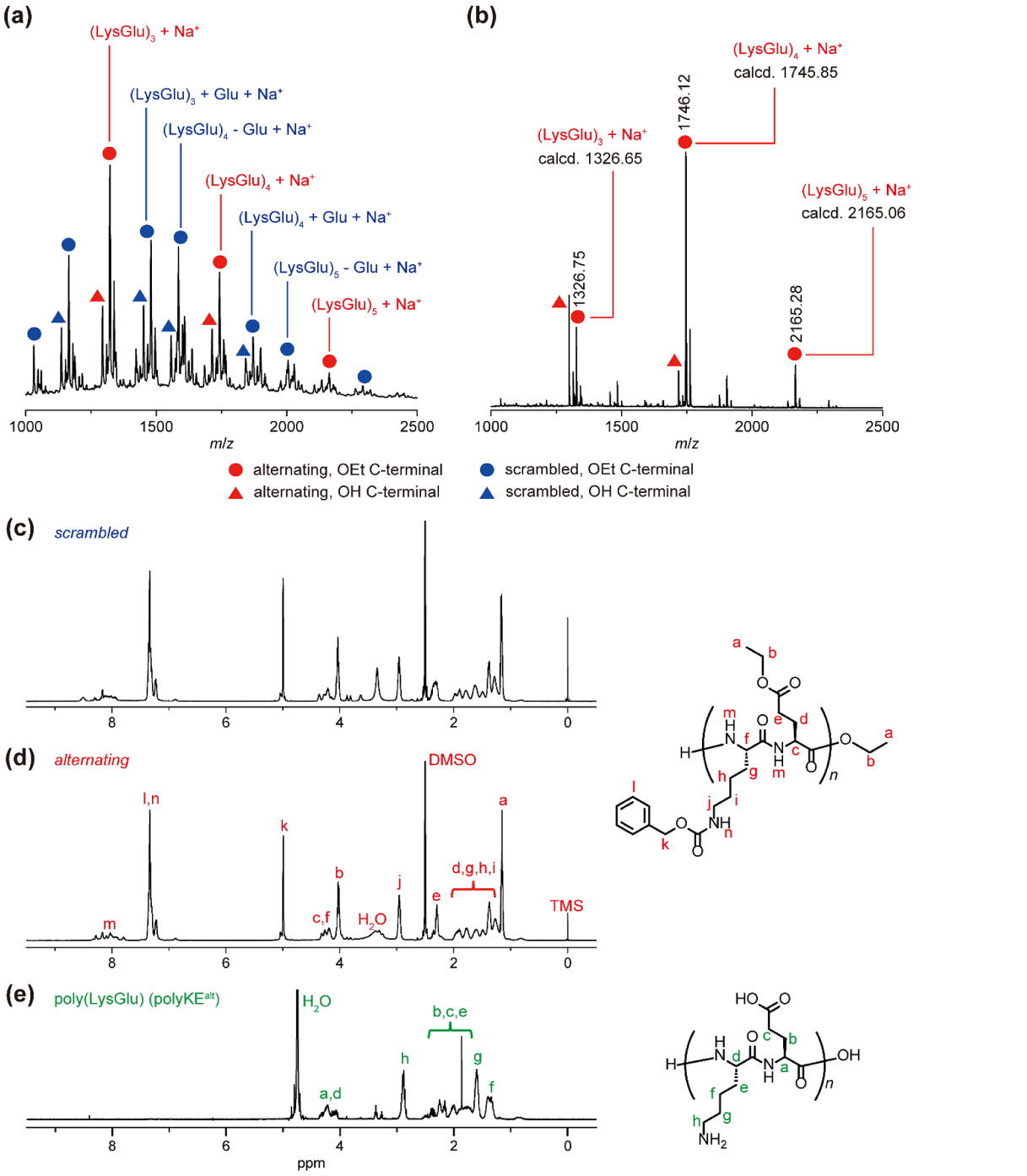

Figure 2. MALDI-TOF MS spectra of poly[Lys(Z)Glu(OEt)] obtained by (a) papain-catalyzed and (b) trypsin-catalyzed polymerization. ^{1}H NMR spectra of poly[Lys(Z)Glu(OEt)] obtained by (c) papain-catalyzed and (d) trypsin-catalyzed polymerizations in DMSO-d_6. (e) The ^{1}H NMR spectrum of polyLysGlu (polyKE^{alt}) in D_2O.

showed almost the same profiles at different pH values from 3 to 10 (Figure 3a). The analysis of secondary structures using a reference data set (DichroWeb) revealed that polyKE^{alt} predominantly adopted a disordered structure with a slight propensity for a helical conformation (Table S1). In contrast, the CD profiles of polyKE^{ran} showed lower molar ellipticity than those of polyKE^{alt}. The CD profiles were almost the same regardless of pH, and the secondary structures tended to be β-strands and turns, as determined from computational analysis (Table S2). This difference was attributed to the inherent randomness of the amino acid sequence. Generally, charged polypeptides such as poly(L-lysine) exhibit structural changes depending on pH.[36,37] The pH independence of the polyKE^{alt} spectrum was due to the ampholytic nature of the equimolar alternating LysGlu sequence.

Ampholytic polypeptides containing Lys and Glu residues have been found to form various self-assembled architectures via electrostatic interactions.[4−8] We performed dynamic light scattering (DLS) analysis to evaluate the self-assembling ability of polyKE^{alt}. The hydrodynamic diameter was estimated by DLS and used to represent the size of the polyKE^{alt} assembly. Once polyKE^{alt} was dissolved in Milli-Q water and vortexed for

https://doi.org/10.1021/acspolymersau.4c00029
ACS Polym. Au 2024, 4, 320−330

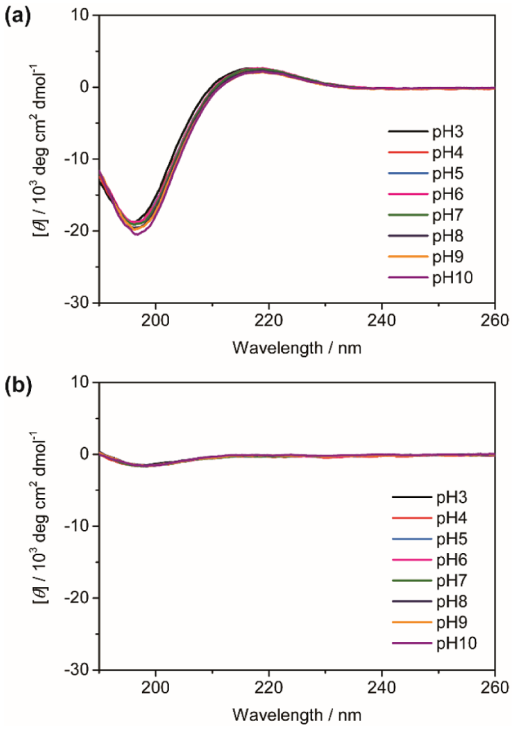

Figure 3. CD spectra of (a) polyKE^{alt} and (b) polyKE^{ran} at various pH values ranging from 3 to 10.

5 s, the peptide spontaneously formed nanosized particles with a size of approximately 100−200 nm (Table S3). This assembly was also formed in both acidic and alkaline solutions, with a slight decrease in the size in the acidic solution. The polyKE^{alt} assembly gradually became larger and aggregated into an insoluble precipitate after a long incubation period of 3 days (Figure S7), indicating the poor long-term stability of the polyKE^{alt} assembly.

To stabilize the polyKE^{alt} assembly, the peptide was modified at the N-terminus with tetra(ethylene glycol) (TEG) (Figure 4a). A TEG carboxylic acid derivative was condensed with poly[Lys(Z)Glu(OEt)], followed by deprotection of the Z and ethyl ester groups, to obtain the TEG-modified peptide TEG-*b*-polyKE^{alt}. The chemical structure of TEG-*b*-polyKE^{alt} was confirmed by MALDI-TOF MS spectrometry and ^{1}H NMR spectroscopy (Figures S8−10). The CD profile of the resulting peptide was similar to that of polyKE^{alt} (Figure S11). The secondary structure of TEG-*b*-polyKE^{alt} was predominantly unordered regardless of pH (Table S4).

TEG-*b*-polyKE^{alt} formed a nanosized assembly with a size of 100−200 nm in Milli-Q water, and the size of the assembly remained almost constant for 24 h (Figure 4b). No aggregates or precipitates were observed after prolonged incubation for more than 1 week, indicating that modification with the TEG moiety significantly increased the stability of the polyKE^{alt}-based assembly.

The morphology of the TEG-*b*-polyKE^{alt} assembly was investigated by field emission scanning electron microscopy (FE-SEM). The assembly was deposited on a silicon substrate and then subjected to FE-SEM, and the results are shown in Figure 4c. The FE-SEM image showed that the TEG-*b*-polyKE^{alt} assembly had a homogeneous spherical morphology and a size ranging from 200 to 300 nm, which was larger than that measured by DLS. The slight increase in size was assumed to be due to flattening of the structure caused by the drying process. To determine whether the assembly adopted a micellar or vesicular morphology, we also performed FE-SEM of a cross section of the TEG-*b*-polyKE^{alt} assembly. The assembly was embedded in epoxy resin and cut into thin slices with a microtome. The cross-sectional FE-SEM image revealed a hollow interior within a spherical structure approximately 100 nm in diameter (Figure 4d), indicating the formation of vesicles from TEG-*b*-polyKE^{alt}. Such a hollow structure has been observed for other previously reported vesicular assemblies by cross-sectional microscopic SEM or TEM observations.[20,24−26,38]

To investigate the effect of the alternating LysGlu sequence on assembly, TEG-modified polyKE^{ran} (TEG-*b*-polyKE^{ran}) was also synthesized (Scheme S3). Because no notable structure was observed via FE-SEM of TEG-*b*-polyKE^{ran}, the assembly morphology of the peptides with alternating or random sequences was observed by atomic force microscopy (AFM). The AFM image of TEG-*b*-polyKE^{alt} exhibited spherical structures, and the size of the assemblies ranged from 100 to 200 nm (Figure 4e). In contrast, the AFM image of TEG-*b*-polyKE^{ran} showed large unordered aggregates as well as a spherical assembly with a broader size distribution (Figure 4f). The height profiles of the assemblies of TEG-*b*-polyKE^{alt} and TEG-*b*-polyKE^{ran} were examined via AFM (Figures S12 and S13). The height of the TEG-*b*-polyKE^{alt} assembly ranged from 4 to 5 nm. The two extended chains of TEG-*b*-polyKE^{alt} with an interdigitated assembly of peptide moieties were approximately 5.9 nm in length (Figure S14), whereas the interdigitated peptide moiety was estimated to be 2.3 nm in length. The sample was dried on a mica substrate for AFM observation, which probably caused the spherical assembly to collapse and the flexible TEG chains to shrink. Therefore, if the TEG-*b*-polyKE^{alt} assembly formed a vesicular structure, the height of the observed assembly would be the sum of two interdigitated peptide layers, namely, 4.6 nm. This estimated value is in good agreement with the heights observed in the AFM images, confirming the formation of polyion complex vesicles assembled from TEG-*b*-polyKE^{alt} through electrostatic interactions between the peptide side chains. The height of the TEG-*b*-polyKE^{ran} assembly was lower, ranging from 0.5 to 1.5 nm (Figure S13), which indicated that TEG-*b*-polyKE^{ran} could not form a rigid interdigitated structure due to the randomness of the peptide sequence.

The stability of the TEG-*b*-polyKE^{ran} assembly was investigated by DLS (Figure S15). The hydrodynamic diameter of the TEG-*b*-polyKE^{ran} assembly estimated by DLS showed a bimodal profile even after a short incubation of 30 min, with one broadened peak with a maximum at approximately 400 nm and another peak at more than several micrometers. The DLS profile became multimodal after a long incubation of up to 24 h. Combined with the AFM observations, these results indicate that TEG-*b*-polyKE^{ran} formed unstable assemblies with a large size distribution.

The self-assembly of TEG-*b*-polyKE^{alt} in various aqueous solutions was investigated by DLS (Figure 4g). The TEG-*b*-polyKE^{alt} assemblies were also stable in phosphate buffer solutions, even at a high concentration of 100 mM, and the average hydrodynamic diameter ranged from 121 to 204 nm. A HEPES buffer solution, the organic component that contains amine and sulfonic acid moieties, allowed the formation of stable assemblies with slightly larger hydrodynamic diameters

https://doi.org/10.1021/acspolymersau.4c00029
ACS Polym. Au 2024, 4, 320−330

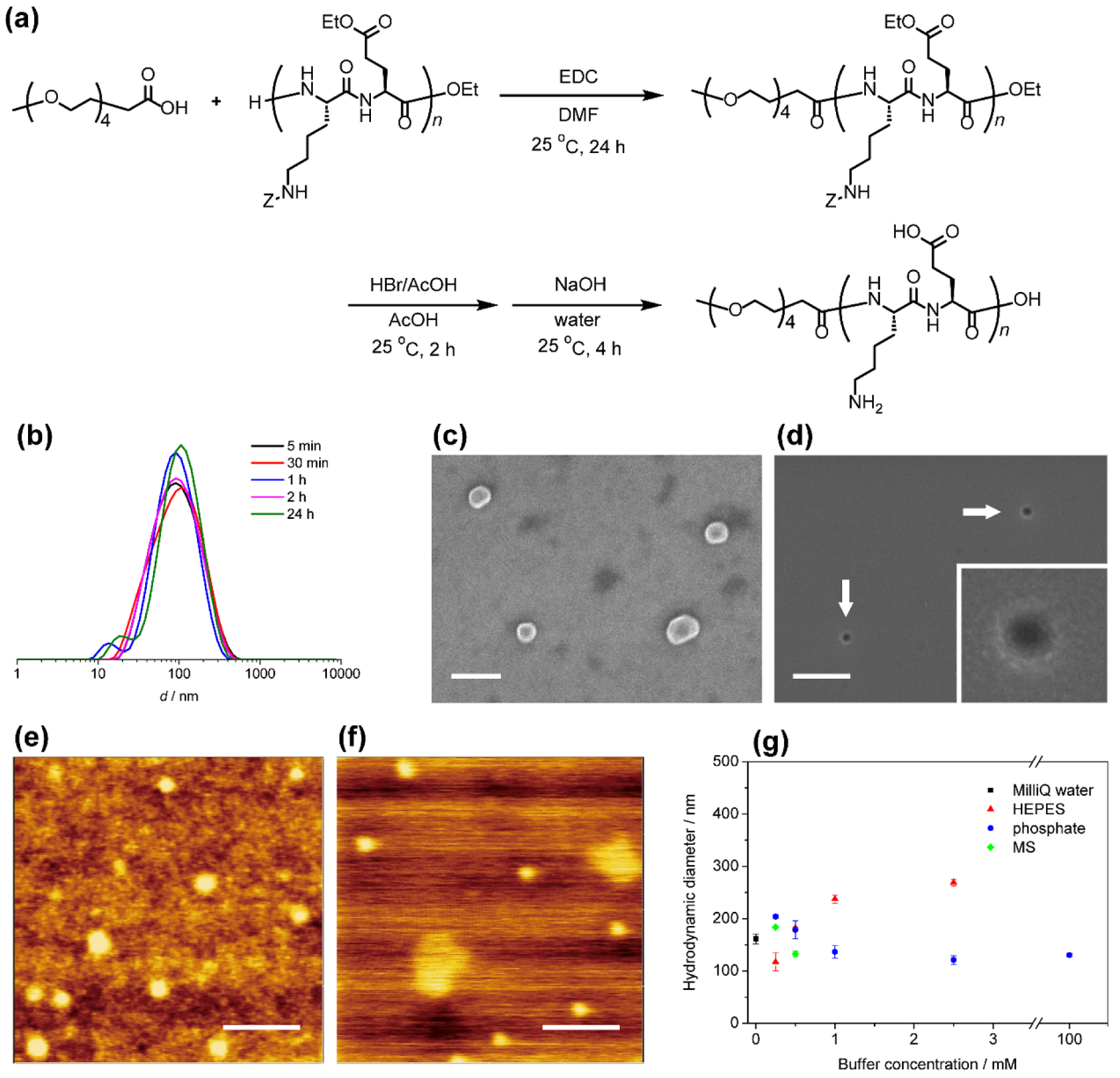

Figure 4. TEG modification of polyKE^{alt} for the formation of stable assemblies. (a) Scheme of the synthesis of TEG-*b*-polyKE^{alt} by condensation with TEG-carboxylic acid and polyKE^{alt} followed by deprotection. (b) DLS profiles of TEG-*b*-polyKE^{alt} in Milli-Q water for 24 h. (c) FE-SEM image of TEG-*b*-polyKE^{alt} deposited on a silicon wafer. (d) Cross-sectional FE-SEM image of a TEG-*b*-polyKE^{alt}-embedded resin. The inset shows a magnified image of a representative assembly. (e, f) AFM topological images of TEG-*b*-polyKE^{alt} (e) and TEG-*b*-polyKE^{ran} (f) deposited on a mica substrate. All scale bars represent 500 nm. (g) The hydrodynamic diameters of the TEG-*b*-polyKE^{alt} assembly estimated by DLS measurements in various buffer solutions. The error bars represent the standard deviation (n = 3). HEPES: 4-(2-hydroxyethyl)piperazine-1-ethanesulfonic acid; MS: Murashige and Skoog culture medium containing 0.25 or 0.5 mM sucrose.

of 237−269 nm at concentrations greater than 1 mM. The hydrodynamic diameter in the HEPES buffer tended to increase with increasing buffer concentration. This result indicated that the electrostatic interaction between TEG-*b*-polyKE^{alt} and the HEPES molecules affected the size of the assembly. We also used Murashige and Skoog (MS) medium, a typical basal medium for plant culture, for DLS measurements because we had previously applied some peptide-based polyion complex vesicles to nanocarriers for material delivery in plant cells.[24−26] The TEG-*b*-polyKE^{alt} assemblies were stable in this MS medium with 0.25 mM and 0.5 mM sucrose, with average hydrodynamic diameters ranging from 133 to 183 nm.

Finally, the ability of TEG-*b*-polyKE^{alt} to encapsulate functional proteins within its hollow region was investigated. As a model protein, the yellow fluorescent protein Citrine[39] was selected for encapsulation in the TEG-*b*-polyKE^{alt} vesicle (Figure 5a). Mixing aqueous solutions of TEG-*b*-polyKE^{alt} and Citrine resulted in the formation of an assembly with a multimodal size distribution (Figure S16). Therefore, Citrine was encapsulated according to a previously reported liposome formation protocol.[40] The solution of Citrine was poured into the membrane of TEG-*b*-polyKE^{alt} deposited at the bottom of a glass vial to encapsulate Citrine. After 3 h of dialysis to remove free Citrine, the resulting solution showed a unimodal size distribution with an average hydrodynamic diameter of

https://doi.org/10.1021/acspolymersau.4c00029
ACS Polym. Au 2024, 4, 320−330

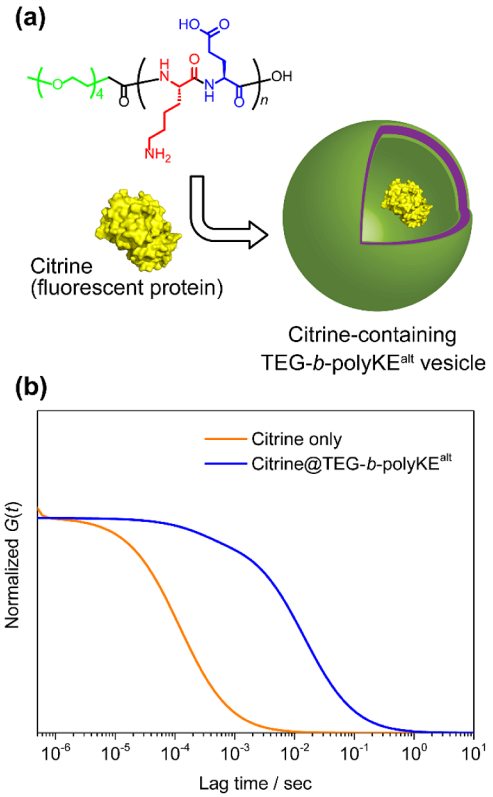

Figure 5. Protein encapsulation in the TEG-*b*-polyKE^{alt} vesicle. (a) Schematic illustration of the encapsulation of a model fluorescent protein (Citrine) in a TEG-*b*-polyKE^{alt} vesicle. (b) Normalized autocorrelation fitting curves obtained by FCS for Citrine (orange) and the Citrine-encapsulated TEG-*b*-polyKE^{alt} vesicle (blue).

140 nm (Figure S16). The size of the assembly was maintained for an additional 24 h of incubation at 25 °C, indicating that no undesired aggregation of TEG-*b*-polyKE^{alt} and Citrine occurred.

The resulting assembly of TEG-*b*-polyKE^{alt} and Citrine was analyzed by fluorescence correlation spectroscopy (FCS) to confirm the encapsulation of Citrine within the hollow region of the TEG-*b*-polyKE^{alt} vesicles. The autocorrelation function $G(t)$ obtained from the FCS measurements of a Citrine solution was fitted using a model of the unimodal fluctuation mode with the kinetics of the transition to a triplet state (Figures S17 and S18).[41] The normalized fitting curves for Citrine with and without TEG-*b*-polyKE^{alt} are shown in Figure 5b. The diffusion coefficient (D) of Citrine was estimated to be 108 μm s^{-1} from the diffusion time (τ) obtained from the $G(t)$ fitting curve for Citrine. The hydrodynamic diameter calculated from D for Citrine was 1.97 nm. In contrast, the $G(t)$ fitting curve for Citrine in the presence of TEG-*b*-polyKE^{alt} showed a remarkable increase in τ, resulting in a smaller D value of 0.899 μm s^{-1}, indicating that the diffusion rate of the fluorescent molecule dramatically decreased due to the size increase caused by encapsulation in the TEG-*b*-polyKE^{alt} vesicles.[24] The hydrodynamic diameter of Citrine-containing TEG-*b*-polyKE^{alt} was calculated to be 238 nm based on the D value, which was slightly greater than that obtained by DLS, probably due to the broad size distribution in the DLS profile (PDI = 0.43). The fluorescence spectrum obtained during the FCS measurements of Citrine was the same in the absence or presence of TEG-*b*-polyKE^{alt}. Citrine has been reported to exhibit spectral changes in response to structural deformation by external stimuli.[42−44] The abovementioned result indicated that undesired interactions and aggregation of Citrine, which would cause structural deformation or denaturation, did not occur in the presence of TEG-*b*-polyKE^{alt}. Therefore, Citrine presumably remained intact within the TEG-*b*-polyKE^{alt} vesicle without any structural deformation.

The remarkable increase in the diffusion time in the FCS analysis clearly indicated the encapsulation of Citrine within the hollow region of the vesicular assembly. In addition, the detection of fluorescence from Citrine in the presence of TEG-*b*-polyKE^{alt} verified that no denaturation of Citrine occurred and that the intact structure of Citrine was maintained even in the TEG-*b*-polyKE^{alt} vesicles. In a control experiment, after mixing the preformed TEG-*b*-polyKE^{alt} solutions with the Citrine solution followed by dialysis (3 h), we could not detect fluorescence from Citrine in the FCS analysis. This result indicated that Citrine was not encapsulated in the TEG-*b*-polyKE^{alt} vesicles after vesicle formation. Citrine has a negative charge on its surface and possibly interacts with positively charged peptides to form a protein/peptide micellar complex via electrostatic interactions.[39,45] However, the dialysis process almost completely eliminated free Citrine from the solution; therefore, no formation of Citrine/peptide complexes was observed in the presence of TEG-*b*-polyKE^{alt}. In contrast, fluorescence from Citrine was detected with a dramatic increase in diffusion time for the sample obtained via the liposome formation protocol. These results collectively indicate that the TEG-*b*-polyKE^{alt} vesicles could encapsulate functional proteins within their hollow space without damaging the structure of the proteins.

CONCLUSIONS

We successfully synthesized ampholytic polypeptides containing an alternating sequence of Lys and Glu residues via chemoenzymatic polymerization. The trypsin-catalyzed polymerization of the Lys(Z)Glu(OEt)-OEt monomer resulted in an alternating sequence without randomization by side reactions such as transamidation. The deprotected peptide with tetra(ethylene glycol) modification, TEG-*b*-polyKE^{alt}, was found to spontaneously form vesicular assemblies with a size of approximately 100−200 nm. The formation of spherical assemblies with a hollow structure was confirmed by FE-SEM and AFM observations. Compared with the sequence of TEG-*b*-polyKE^{ran}, the alternating sequence of Lys and Glu is highly important for the stability of assemblies with relatively small sizes and size distributions. The FCS measurement indicated that the TEG-*b*-polyKE^{alt} vesicle assumedly encapsulated the yellow fluorescent model protein Citrine without disrupting its functional structure, demonstrating the potential of the vesicle as a nanocarrier for material delivery. The peptide bonds of TEG-*b*-polyKE^{alt} are labile to proteolytic degradation, which will allow for proteolysis-triggered release in material delivery applications. The spontaneous generation of vesicle architecture by ampholytic TEG-*b*-polyKE^{alt} underscores the significance of this facile process with promising implications for future applications, including material delivery systems and nanoreactors.

https://doi.org/10.1021/acspolymersau.4c00029
ACS Polym. Au 2024, 4, 320−330

EXPERIMENTAL AND METHODS

Materials

Papain (EC No. 3.4.22.2) was purchased from Wako Pure Chemical Industries Ltd. (Osaka, Japan) and was used as received. The activity was approximately 0.5 U g^{-1}, where one unit hydrolyzes 1 mmol of *N*-benzoyl-DL-arginine *p*-nitroanilide per minute at pH 7.5 and 25 °C. Trypsin (EC No. 3.4.21.4) was purchased from Sigma−Aldrich (St. Louis, USA). The activity was 1000−2000 U mg^{-1} based on the *N*-benzoyl-L-arginine ethyl ester hydrochloride (BAEE) test. Amino acid derivatives and 1-(3-(dimethylamino)propyl)-3-ethylacarbodiimide (EDC) HCl salt were purchased from Watanabe Chemical Industries Ltd. (Hiroshima, Japan) and were used as received. The other chemicals were purchased from Tokyo Chemical Industry Co. Ltd. (Tokyo, Japan) and were used as received without purification unless otherwise noted. Carboxylated tetra(ethylene glycol) with a methoxy terminal group (TEG-COOH) was synthesized according to a previously reported procedure with slight modifications (Scheme S4).[46] The yellow fluorescent protein Citrine was synthesized by a dialysis-mode cell-free protein synthesis method according to a previous study.[39] The stock solution of Citrine in 10 mM Tris buffer (pH 8.0) was diluted 100-fold with Milli-Q water prior to encapsulation experiments.

Synthesis of Boc-Lys(Boc)Glu(OEt)-OEt

To a 200 mL flask equipped with a stir bar and an additional funnel were added Boc-L-Lys(Boc)−OH (5.00 g, 14.4 mmol), L-Glu(OEt)-OEt HCl salt (3.46 g, 14.4 mmol), 1-hydroxybenzotriazole (HOBt) monohydrate (2.21 g, 14.4 mmol), and chloroform (25 mL) under nitrogen. Triethylamine (2.0 mL, 14.4 mmol) was added to the mixture at 0 °C. Then, a solution of EDC HCl salt (2.76 g, 14.4 mmol) in chloroform was added dropwise at 0 °C, and the mixture was stirred at 25 °C for 24 h. After the reaction, the solution was washed with 5% $NaHCO_3$ aqueous solution three times and saturated brine. The organic layer was dried with $MgSO_4$ and concentrated by means of a rotary evaporator. After drying under vacuum, a white solid was obtained. The yield was 7.46 g (97%).

Synthesis of LysGlu(oet)-OEt HCl Salt

To a solution of Boc-Lys(Boc)Glu(OEt)-OEt (7.46 g, 14.0 mmol) in dichloromethane (20 mL), trifluoroacetic acid (TFA, 20 mL) was added in a 100 mL flask equipped with a stir bar, and the mixture was stirred at 25 °C for 6 h. After the reaction, the solvent was removed by means of a rotary evaporator. Dioxane/HCl (4 M, 8 mL) was added to the resulting viscous liquid, and the solution was poured into excess diethyl ether. The precipitate was filtered, washed with diethyl ether, and dried under vacuum to afford a white solid. The yield was 5.5 g (98%).

Synthesis of Boc-Lys(Z)Glu(OEt)-OEt

The title compound was synthesized in a manner similar to that applied for Boc-Lys(Boc)Glu(OEt)-OEt from Boc-L-Lys(Z)−OH (5.00 g, 13.1 mmol) and L-Glu(OEt)-OEt HCl salt (3.14 g, 13.1 mmol). The yield was 6.94 g (94%).

Synthesis of Lys(Z)Glu(OEt)-OEt HCl Salt

The title compound was synthesized in a manner similar to that applied for LysGlu(OEt)-OEt from Boc-Lys(Z)Glu(OEt)-OEt (6.90 g, 12.2 mmol). A white solid was obtained. The yield was 6.0 g (98%).

Protease-Catalyzed Polymerization of LysGlu Monomers

Chemoenzymatic polymerization of two types of LysGlu monomers was carried out using papain or trypsin as the enzyme catalyst. As a representative procedure, the trypsin-catalyzed polymerization of the Lys(Z)Glu(OEt)-OEt monomer was as follows. Lys(Z)Glu(OEt)-OEt HCl salt (0.502 g, 1.0 mmol) was dissolved in 1 M phosphate buffer (pH 8.0, 2 mL) in a 25 mL glass tube, and the solution was stirred at 40 °C. A solution of trypsin (0.200 g) in phosphate buffer (1 mL) was added in one portion to this solution, and the mixture was stirred at 40 °C and 800 rpm for 2 h. The final concentrations of the dipeptide monomer and enzyme were 0.1 M and 50 mg mL^{-1}, respectively. After cooling to 25 °C, the precipitate was collected by centrifugation at 9000 rpm for 15 min. The collected pellet was washed with Milli-Q water twice and lyophilized to afford poly[Lys(Z)Glu(OEt)] as a white solid. The yield was 0.383 g (91.3%).

Synthesis of PolyKE^{alt} by Deprotection of Poly[Lys(Z)Glu(OEt)]

Poly[Lys(Z)Glu(OEt)] (0.273 g) was dissolved in an HBr solution in acetic acid (5.1 M, 5 mL), and the mixture was stirred at 25 °C for 2 h. Then, the solution was poured into excess diethyl ether, and the precipitate was filtered, washed with diethyl ether, and dried under vacuum. The solid was then dissolved in an aqueous NaOH solution (5 M, 4 mL), and the mixture was stirred at 25 °C for 12 h. The solution was then neutralized with 6 M HCl and dialyzed against Milli-Q water at 25 °C for 6 h using a CE tube (Spectra/Por CE, MWCO: 100−500 Da). After dialysis, the solution was lyophilized to afford the deprotected polyLysGlu (polyKE^{alt}) as a white powder. The yield was 0.153 g (91%).

Synthesis of TEG-*b*-PolyKE^{alt}

To a solution of poly[Lys(Z)Glu(OEt)] (0.851 g, 0.494 mmol) and TEG-COOH (0.248 g, 0.988 mmol) in dehydrated dimethylformamide (6 mL) was added EDC HCl salt (0.189 g, 0.988 mmol). The mixture was stirred at 25 °C for 24 h. After the reaction, the solution was poured into excess water. The precipitate was collected by centrifugation (9000 rpm, 15 min), washed with water twice, and lyophilized to afford the TEG-conjugated peptide TEG-*b*-poly[Lys(Z)Glu(OEt)] as a white powder. Deprotection of TEG-*b*-poly[Lys(Z)Glu(OEt)] was carried out by the same procedure used for poly[Lys(Z)Glu(OEt)] as described above to afford TEG-*b*-polyLysGlu (TEG-*b*-polyKE^{alt}). The yield was 0.762 g.

Analyses

The IR spectra of the bulk samples were recorded on an IRPrestige-21 Fourier transform IR spectrophotometer (Shimadzu Corporation, Kyoto, Japan) with a MIRacle A single-reflection attenuated total reflectance (ATR) unit using a Ge prism. The ^1H NMR spectra were recorded on a JNM-EX270 FT NMR system (JEOL Ltd., Tokyo, Japan) at 25 °C at 270 MHz. Chloroform-*d*, deuterated dimethyl sulfoxide (DMSO-d_6), or deuterium oxide was used as the solvent, and tetramethylsilane (TMS) served as an internal standard. Matrix-assisted laser desorption/ionization time-of-flight (MALDI-TOF) mass spectrometric analysis was conducted using an ultrafleXtreme MALDI-TOF spectrophotometer (Bruker Daltonics, Billerica, MA) operating in reflection mode at an accelerating voltage of 15 kV. The sample was dissolved in water/acetonitrile (0.8 mg mL^{-1}) containing 0.1% TFA mixed with a solution of α-cyano-4-hydroxycinnamic acid (CHCA) in water/acetonitrile (10 mg mL^{-1}) and deposited on an MTP 384 ground steel BC target plate.

Circular Dichroism (CD) Measurements

CD spectra of the peptide samples were recorded on a JASCO J-820 spectropolarimeter. A quartz cuvette with a 0.1 cm path length was used for the measurements. The peptides were dissolved in Milli-Q water at 0.5 mM. The CD spectroscopic data were analyzed by means of DichroWeb, an online server for protein secondary structure analyses, using the CONTIN-LL algorithm[47] with reference data set 7 to estimate the contents of the secondary structures.[48,49]

Field Emission Scanning Electron Microscopy (FE-SEM)

An aqueous solution of TEG-*b*-polyKE^{alt} (250 μM) was dropped on a silicon wafer and dried in vacuo. The sample on the wafer was subjected to FE-SEM observation by a GeminiSEM 300 (Carl Zeiss, Oberkochen, Germany) with an acceleration voltage of 1 kV. The sliced sample for observation of the cross section was prepared as follows.[26] TEG-*b*-polyKE^{alt} was dissolved in Milli-Q water (250 μM), and 200 μL of the solution was slowly mixed with melted agarose gel (200 μM) at 30 °C. After cooling to 25 °C, the fixed gel was cut into small pieces (approximately 1 × 1 mm^2). The gel sample was dehydrated by gradual solvent substitution with methanol to propylene oxide to Epon 812 (TAAB Laboratories Equipment Ltd., Berkshire, UK). The agarose gel was finally embedded in an epoxy

https://doi.org/10.1021/acspolymersau.4c00029
ACS Polym. Au 2024, 4, 320−330

resin by curing the Epon 812-swollen gel at 60 °C for 48 h. The solidified sample was cut into a thin 100 nm thick slice by an ultramicrotome ATUMtome (RMC-Boechele, AZ) and used for cross-sectional FE-SEM observation.

Dynamic Light Scattering (DLS) Measurements

The size of the assemblies formed from TEG-*b*-polyKE^{alt} was evaluated by DLS using a Zetasizer Nano ZS instrument (Malvern Instruments Ltd., Worcestershire, UK). After TEG-*b*-polyKE^{alt} was dissolved in Milli-Q water, the solution was vortexed for 5 s, filtered through a membrane filter (45 μm), and incubated at 25 °C for the indicated times. The solution was placed in a plastic cell (DTS1070) and subjected to DLS measurements using a 633 nm He−Ne laser at 25 °C with a backscatter detection angle of 173° to estimate the hydrodynamic diameter and zeta potential. The z-averaged mean size was calculated as the hydrodynamic diameter by analyzing the obtained autocorrelation function by cumulant method with a single exponential analysis using ISO13321 for normalization. The multimodal size distribution was analyzed by non-negative linear least-squares (NNLS) method. The measurements were replicated three times, and the data were averaged to determine the standard deviation. Phosphate buffer (0.25−100 mM, pH 7.4), 4-(2-hydroxyethyl)piperazine-1-ethanesulfonic acid (HEPES) buffer (0.25−2.5 mM, pH 7.4), and Murashige and Skoog (MS) medium (0.25−0.5 mM sucrose, pH 5.7) were also used for DLS measurements of the TEG-*b*-polyKE^{alt} assemblies. The MS medium was prepared from half-strength MS Basal Medium powder (Sigma-Aldrich, Missouri, USA), and the concentration of sucrose was adjusted to 0.25 or 0.5 mM.

Atomic Force Microscopy (AFM)

The morphology of the assemblies formed from TEG-*b*-polyKE^{alt} and TEG-*b*-polyKE^{ran} was investigated by AFM. The peptides were dissolved in Milli-Q water (1 mg mL^{-1}), and the solution was incubated at 25 °C for 1 h. An aliquot (10 μL) of the solution was deposited on a mica substrate and dried under vacuum. The sample was then subjected to AFM observation using an AFM5300E (Hitachi High-Tech Science Corporation, Tokyo, Japan) in dynamic force mode with SI-DF3 cantilevers (force constant: 1.6 N m^{-1}, resonance frequency: 26 kHz). Topological images of the assemblies were obtained at 25 °C by AFM observation of the TEG-*b*-polyKE^{alt} and TEG-*b*-polyKE^{ran} samples.

Fluorescence Correlation Spectroscopy (FCS)

FCS measurements of a Citrine aqueous solution with and without the TEG-*b*-polyKE^{alt} vesicle were performed. The Citrine-containing TEG-*b*-polyKE^{alt} sample was prepared according to the liposome formation protocol.[40] Prior to the encapsulation of Citrine, TEG-*b*-polyKE^{alt} was dissolved in chloroform/methanol and placed in a 10 mL vial. After the solvent was completely evaporated, the aqueous solution of Citrine (27 μg mL^{-1}) was poured into the peptide-coated vial and vortexed for 10 s. The sample was incubated at 25 °C for 5 min and then dialyzed against Milli-Q water for 3 h using a CE tube (MWCO: 100 kDa) to remove free Citrine. The resulting solution sample was then used for FCS measurements using an LSM880 confocal laser microscope (Carl Zeiss) with a 488 nm laser at 25 °C. The autocorrelation function $G(t)$ curves obtained by means of ZEN 2.3 SP1 operating software (Carl Zeiss) were subjected to fitting by a model function including singlet−triplet kinetics using the following equation:[41]

$$G(t) = 1 + \frac{1}{N}\left(1 + \frac{t}{\tau}\right)^{-1}\left(1 + \frac{t}{k^2\tau}\right)^{-1/2}\left(\frac{1 - F + Fe^{t/\tau_T}}{1 - F}\right)$$

where N is the number of fluorescent molecules, t is the correlation time, τ is the diffusion time of the component, k is a structural constant, F is the average fraction of fluorescent species present in the triplet state, and τ_T is the characteristic triplet correlation time. The diffusion coefficient D was calculated from τ using rhodamine 6G as a standard. The hydrodynamic diameter R was estimated from D using the Stokes−Einstein equation:

$$D = \frac{k_B T}{3\pi\eta R}$$

where k_B is the Boltzmann constant, T is the measuring temperature, and η is the viscosity of the solvent.

ASSOCIATED CONTENT

Supporting Information

The Supporting Information is available free of charge at https://pubs.acs.org/doi/10.1021/acspolymersau.4c00029.

Synthetic schemes for monomer and polymer syntheses; ^{1}H NMR spectra of products; MALDI-TOF mass spectra of the polyKE derivatives; a photo of polyKE^{alt} aggregates; CD spectra and secondary structure propensity of polyKE derivatives; AFM height profiles of TEG-*b*-polyKE; molecular structure of TEG-*b*-polyKE^{alt}; DLS profiles of TEG-*b*-polyKE; experimental autocorrelation functions and fitting curves (PDF)

AUTHOR INFORMATION

Corresponding Authors

Kousuke Tsuchiya − *Department of Material Chemistry, Graduate School of Engineering, Kyoto University, Kyoto 615-8510, Japan; Department of Chemistry and Biotechnology, School of Engineering, The University of Tokyo, Bunkyo-ku, Tokyo 113-8656, Japan; Biomacromolecules Research Team, RIKEN Center for Sustainable Resource Science, Wako, Saitama 351-0198, Japan;* orcid.org/0000-0003-2364-8275; Phone: +81-3-5841-1899; Email: ktsuchiya@gel.t.u-tokyo.ac.jp

Keiji Numata − *Department of Material Chemistry, Graduate School of Engineering, Kyoto University, Kyoto 615-8510, Japan; Biomacromolecules Research Team, RIKEN Center for Sustainable Resource Science, Wako, Saitama 351-0198, Japan;* orcid.org/0000-0003-2199-7420; Phone: +81-75-383-2400; Email: keiji.numata@riken.jp

Author

Seiya Fujita − *Department of Material Chemistry, Graduate School of Engineering, Kyoto University, Kyoto 615-8510, Japan*

Complete contact information is available at: https://pubs.acs.org/10.1021/acspolymersau.4c00029

Author Contributions

K.T. and K.N. conceived and designed the research. K.T. and S.F. performed the experiments and analyzed the data. K.T. wrote the manuscript, and K.T. and K.N. edited the manuscript. CRediT: **Kousuke Tsuchiya** conceptualization, data curation, formal analysis, investigation, methodology, resources, validation, visualization, writing-original draft, writing-review & editing; **Seiya Fujita** formal analysis, investigation, methodology; **Keiji Numata** conceptualization, funding acquisition, investigation, methodology, project administration, resources, supervision, validation, writing-review & editing.

Funding

This work was supported by Japan Science and Technology Agency (JST) Exploratory Research for Advanced Technology (ERATO) Grant No. JPMJER1602, JST PRESTO Grant No. JPMJPR21N6, Grant-in-Aid for Transformative Research

Areas (B) Grant No. JP20H05735, JSPS KAKENHI Grant No. JP20K05636, JST COI-NEXT, and the MEXT Program: Data Creation and Utilization-Type Material Research and Development Project Grant Number JPMXP1122714694.

Notes

The authors declare no competing financial interest.

■ ACKNOWLEDGMENTS

We acknowledge Dr. Takanori Kigawa and Ms. Yoko Motoda for the cell-free synthesis of the yellow fluorescent protein Citrine.

■ REFERENCES

(1) Ji, T. H.; Grossmann, M.; Ji, I. G Protein-coupled Receptors: I. DIVERSITY OF RECEPTOR-LIGAND INTERACTIONS*. *J. Biol. Chem.* **1998**, *273* (28), 17299−17302.
(2) Cygler, M.; Schrag, J. D.; Sussman, J. L.; Harel, M.; Silman, I.; Gentry, M. K.; Doctor, B. P. Relationship between sequence conservation and three-dimensional structure in a large family of esterases, lipases, and related proteins. *Protein Sci.* **1993**, *2* (3), 366−382.
(3) Landschulz, W. H.; Johnson, P. F.; McKnight, S. L. The Leucine Zipper: A Hypothetical Structure Common to a New Class of DNA Binding Proteins. *Science* **1988**, *240* (4860), 1759−1764.
(4) Miki, T.; Nakai, T.; Hashimoto, M.; Kajiwara, K.; Tsutsumi, H.; Mihara, H. Intracellular artificial supramolecules based on de novo designed Y15 peptides. *Nat. Commun.* **2021**, *12* (1), 3412.
(5) Ye, H.; Che, J.; Huang, R.; Qi, W.; He, Z.; Su, R. Zwitterionic Peptide Enhances Protein-Resistant Performance of Hyaluronic Acid-Modified Surfaces. *Langmuir* **2020**, *36* (8), 1923−1929.
(6) Kim, J. H.; Kim, S. C.; Kline, M. A.; Grzincic, E. M.; Tresca, B. W.; Cardiel, J.; Karbaschi, M.; Dehigaspitiya, D. C.; Chen, Y.; Udumula, V.; et al. Discovery of Stable and Selective Antibody Mimetics from Combinatorial Libraries of Polyvalent, Loop-Functionalized Peptoid Nanosheets. *ACS Nano* **2020**, *14* (1), 185−195.
(7) Yu, Z.; Cai, Z.; Chen, Q.; Liu, M.; Ye, L.; Ren, J.; Liao, W.; Liu, S. Engineering β-sheet peptide assemblies for biomedical applications. *Biomater. Sci.* **2016**, *4* (3), 365−374.
(8) Zhang, S.; Holmes, T.; Lockshin, C.; Rich, A. Spontaneous assembly of a self-complementary oligopeptide to form a stable macroscopic membrane. *Proc. Nat. Acad. Sci.* **1993**, *90* (8), 3334−3338.
(9) Mi, L.; Jiang, S. Integrated Antimicrobial and Nonfouling Zwitterionic Polymers. *Angew. Chem., Int. Ed.* **2014**, *53* (7), 1746−1754.
(10) Iwasaki, Y.; Ishihara, K. Phosphorylcholine-containing polymers for biomedical applications. *Anal. Bioanal. Chem.* **2005**, *381* (3), 534−546.
(11) Lowe, A. B.; McCormick, C. L. Synthesis and Solution Properties of Zwitterionic Polymers. *Chem. Rev.* **2002**, *102* (11), 4177−4190.
(12) White, A. D.; Nowinski, A. K.; Huang, W.; Keefe, A. J.; Sun, F.; Jiang, S. Decoding nonspecific interactions from nature. *Chem. Sci.* **2012**, *3* (12), 3488−3494.
(13) Yuan, Z.; Li, B.; Niu, L.; Tang, C.; McMullen, P.; Jain, P.; He, Y.; Jiang, S. Zwitterionic Peptide Cloak Mimics Protein Surfaces for Protein Protection. *Angew. Chem., Int. Ed.* **2020**, *59* (50), 22378−22381.
(14) Trital, A.; Xue, W.; Chen, S. Development of a Negative-Biased Zwitterionic Polypeptide-Based Nanodrug Vehicle for pH-Triggered Cellular Uptake and Accelerated Drug Release. *Langmuir* **2020**, *36* (26), 7181−7189.
(15) Smith, J.; McMullen, P.; Yuan, Z.; Pfaendtner, J.; Jiang, S. Elucidating Molecular Design Principles for Charge-Alternating Peptides. *Biomacromolecules* **2020**, *21* (2), 435−443.
(16) Qi, H.; Zheng, W.; Zhou, X.; Zhang, C.; Zhang, L. A mussel-inspired chimeric protein as a novel facile antifouling coating. *Chem. Commun.* **2018**, *54* (80), 11328−11331.
(17) Yang, Q.; Wang, L.; Lin, W.; Ma, G.; Yuan, J.; Chen, S. Development of nonfouling polypeptides with uniform alternating charges by polycondensation of the covalently bonded dimer of glutamic acid and lysine. *J. Mater. Chem. B* **2014**, *2* (5), 577−584.
(18) Nowinski, A. K.; Sun, F.; White, A. D.; Keefe, A. J.; Jiang, S. Sequence, Structure, and Function of Peptide Self-Assembled Monolayers. *J. Am. Chem. Soc.* **2012**, *134* (13), 6000−6005.
(19) Cabral, H.; Miyata, K.; Osada, K.; Kataoka, K. Block Copolymer Micelles in Nanomedicine Applications. *Chem. Rev.* **2018**, *118* (14), 6844−6892.
(20) Chen, H.; Xiao, L.; Anraku, Y.; Mi, P.; Liu, X.; Cabral, H.; Inoue, A.; Nomoto, T.; Kishimura, A.; Nishiyama, N.; et al. Polyion Complex Vesicles for Photoinduced Intracellular Delivery of Amphiphilic Photosensitizer. *J. Am. Chem. Soc.* **2014**, *136* (1), 157−163.
(21) Anraku, Y.; Kishimura, A.; Oba, M.; Yamasaki, Y.; Kataoka, K. Spontaneous Formation of Nanosized Unilamellar Polyion Complex Vesicles with Tunable Size and Properties. *J. Am. Chem. Soc.* **2010**, *132* (5), 1631−1636.
(22) Kishimura, A.; Koide, A.; Osada, K.; Yamasaki, Y.; Kataoka, K. Encapsulation of Myoglobin in PEGylated Polyion Complex Vesicles Made from a Pair of Oppositely Charged Block Ionomers: A Physiologically Available Oxygen Carrier. *Angew. Chem., Int. Ed.* **2007**, *46* (32), 6085−6088.
(23) Koide, A.; Kishimura, A.; Osada, K.; Jang, W.-D.; Yamasaki, Y.; Kataoka, K. Semipermeable Polymer Vesicle (PICsome) Self-Assembled in Aqueous Medium from a Pair of Oppositely Charged Block Copolymers: Physiologically Stable Micro-/Nanocontainers of Water-Soluble Macromolecules. *J. Am. Chem. Soc.* **2006**, *128* (18), 5988−5989.
(24) Odahara, M.; Watanabe, K.; Kawasaki, R.; Tsuchiya, K.; Tateishi, A.; Motoda, Y.; Kigawa, T.; Kodama, Y.; Numata, K. Nanoscale Polyion Complex Vesicles for Delivery of Cargo Proteins and Cas9 Ribonucleoprotein Complexes to Plant Cells. *ACS Appl. Nano Mater.* **2021**, *4* (6), 5630−5635.
(25) Fujita, S.; Tsuchiya, K.; Numata, K. All-Peptide-Based Polyion Complex Vesicles: Facile Preparation and Encapsulation of the Protein in Active Form. *ACS Polym. Au* **2021**, *1* (1), 30−38.
(26) Fujita, S.; Motoda, Y.; Kigawa, T.; Tsuchiya, K.; Numata, K. Peptide-Based Polyion Complex Vesicles That Deliver Enzymes into Intact Plants To Provide Antibiotic Resistance without Genetic Modification. *Biomacromolecules* **2021**, *22* (3), 1080−1090.
(27) Terada, K.; Kurita, T.; Gimenez-Dejoz, J.; Masunaga, H.; Tsuchiya, K.; Numata, K. Papain-Catalyzed, Sequence-Dependent Polymerization Yields Polypeptides Containing Periodic Histidine Residues. *Macromolecules* **2022**, *55* (16), 6992−7002.
(28) Gudeangadi, P. G.; Tsuchiya, K.; Sakai, T.; Numata, K. Chemoenzymatic synthesis of polypeptides consisting of periodic di- and tri-peptide motifs similar to elastin. *Polym. Chem.* **2018**, *9* (17), 2336−2344.
(29) Tsuchiya, K.; Numata, K. Chemoenzymatic synthesis of polypeptides containing the unnatural amino acid 2-aminoisobutyric acid. *Chem. Commun.* **2017**, *53* (53), 7318−7321.
(30) Qin, X.; Xie, W.; Tian, S.; Cai, J.; Yuan, H.; Yu, Z.; Butterfoss, G. L.; Khuong, A. C.; Gross, R. A. Enzyme-triggered hydrogelation via self-assembly of alternating peptides. *Chem. Commun.* **2013**, *49* (42), 4839−4841.
(31) Qin, X.; Khuong, A. C.; Yu, Z.; Du, W.; Decatur, J.; Gross, R. A. Simplifying alternating peptide synthesis by protease-catalyzed dipeptide oligomerization. *Chem. Commun.* **2013**, *49* (4), 385−387.
(32) Tsuchiya, K.; Numata, K. Chemoenzymatic Synthesis of Polypeptides for Use as Functional and Structural Materials. *Macromol. Biosci.* **2017**, *17* (11), 1700177.
(33) Miyamoto, T.; Tsuchiya, K.; Numata, K. Block Copolymer/Plasmid DNA Micelles Postmodified with Functional Peptides via

Thiol−Maleimide Conjugation for Efficient Gene Delivery into Plants. *Biomacromolecules* **2019**, *20* (2), 653−661.
(34) Qin, X.; Xie, W.; Su, Q.; Du, W.; Gross, R. A. Protease-Catalyzed Oligomerization of l-Lysine Ethyl Ester in Aqueous Solution. *ACS Catal.* **2011**, *1* (9), 1022−1034.
(35) Uyama, H.; Fukuoka, T.; Komatsu, I.; Watanabe, T.; Kobayashi, S. Protease-Catalyzed Regioselective Polymerization and Copolymerization of Glutamic Acid Diethyl Ester. *Biomacromolecules* **2002**, 3 (2), 318−323.
(36) Kambara, O.; Tamura, A.; Naito, A.; Tominaga, K. Structural changes of poly-l-lysine in solution and lyophilized form. *Phys. Chem. Chem. Phys.* **2008**, *10* (33), 5042−5044.
(37) Arunkumar, A. I.; Kumar, T. K. S.; Yu, C. Specificity of helix-induction by 2,2,2-trifluoroethanol in polypeptides. *Int. J. Biol. Macromol.* **1997**, *21* (3), 223−230.
(38) Ke, W.; Li, J.; Mohammed, F.; Wang, Y.; Tou, K.; Liu, X.; Wen, P.; Kinoh, H.; Anraku, Y.; Chen, H.; et al. Therapeutic Polymersome Nanoreactors with Tumor-Specific Activable Cascade Reactions for Cooperative Cancer Therapy. *ACS Nano* **2019**, *13* (2), 2357−2369.
(39) Ng, K. K.; Motoda, Y.; Watanabe, S.; Sofiman Othman, A.; Kigawa, T.; Kodama, Y.; Numata, K. Intracellular Delivery of Proteins via Fusion Peptides in Intact Plants. *PLoS One* **2016**, *11* (4), No. e0154081.
(40) Bulbake, U.; Doppalapudi, S.; Kommineni, N.; Khan, W. Liposomal Formulations in Clinical Use: An Updated Review. *Pharmaceutics* **2017**, *9* (2), 12.
(41) Widengren, J.; Mets, U.; Rigler, R. Fluorescence correlation spectroscopy of triplet states in solution: A theoretical and experimental study. *J. Phys. Chem.* **1995**, *99* (36), 13368−13379.
(42) Barstow, B.; Ando, N.; Kim, C. U.; Gruner, S. M. Alteration of citrine structure by hydrostatic pressure explains the accompanying spectral shift. *Proc. Nat. Acad. Sci.* **2008**, *105* (36), 13362−13366.
(43) McAnaney, T. B.; Zeng, W.; Doe, C. F. E.; Bhanji, N.; Wakelin, S.; Pearson, D. S.; Abbyad, P.; Shi, X.; Boxer, S. G.; Bagshaw, C. R. Protonation, Photobleaching, and Photoactivation of Yellow Fluorescent Protein (YFP 10C): A Unifying Mechanism. *Biochemistry* **2005**, *44* (14), 5510−5524.
(44) Heikal, A. A.; Hess, S. T.; Baird, G. S.; Tsien, R. Y.; Webb, W. W. Molecular spectroscopy and dynamics of intrinsically fluorescent proteins: Coral red (dsRed) and yellow (Citrine). *Proc. Nat. Acad. Sci.* **2000**, *97* (22), 11996−12001.
(45) Guo, B.; Itami, J.; Oikawa, K.; Motoda, Y.; Kigawa, T.; Numata, K. Native protein delivery into rice callus using ionic complexes of protein and cell-penetrating peptides. *PLoS One* **2019**, *14* (7), No. e0214033.
(46) Taubitz, J.; Lüning, U. On the Importance of the Nature of Hydrogen Bond Donors in Multiple Hydrogen Bond Systems. *Eur. J. Org. Chem.* **2008**, *2008* (35), 5922−5927.
(47) Miles, A. J.; Ramalli, S. G.; Wallace, B. A. DichroWeb, a website for calculating protein secondary structure from circular dichroism spectroscopic data. *Protein Sci.* **2022**, *31* (1), 37−46.
(48) Sreerama, N.; Woody, R. W. Estimation of Protein Secondary Structure from Circular Dichroism Spectra: Comparison of CONTIN, SELCON, and CDSSTR Methods with an Expanded Reference Set. *Anal. Biochem.* **2000**, *287* (2), 252−260.
(49) Sreerama, N.; Venyaminov, S. Y. U.; Woody, R. W. Estimation of the number of α-helical and β-strand segments in proteins using circular dichroism spectroscopy. *Protein Sci.* **1999**, *8* (2), 370−380.

https://doi.org/10.1021/acspolymersau.4c00029
ACS Polym. Au 2024, 4, 320−330